Dedicated to Professor Dr.- Ing. Georg Frommeyer on the occasion of his 65th birthday

Characterization of Reverted Austenite during Prolonged Ageing of Maraging Steel *CORRAX*

S. Höring[1], D. Abou-Ras[1], N. Wanderka[1], H. Leitner[2], H. Clemens[2], J. Banhart[1],

[1]Helmholtz Centre Berlin, Glienickerstr. 100, 14109 Berlin, Germany

[2]University of Leoben, Department of Physical Metallurgy and Materials Testing, Franz-Josef-Str. 18, 8700 Leoben, Austria

Abstract

Microstructure and mechanical properties have been studied in *CORRAX* maraging steel during prolonged ageing up to 300 h at 798 K. Strengthening of maraging steel was caused by the formation of an intermetallic phase enriched in Ni and Al that is an ordered B2 (CsCl) superlattice structure. Precipitation hardening was accompanied by an increase in micro-hardness with peak hardness after about 12 h of ageing. After 300 h of ageing, the micro-hardness value is still high, corresponding to 94% of the peak hardness. The reverse transformation of martensite to austenite does practically not take place during prolonged ageing as shown by X-ray and electron backscatter diffraction (EBSD) analysis. The experimentally determined amount of austenite (1-2 vol.%) is in good agreement with the calculated value (about 2.5 vol.%).

Keywords: Corrax, reverted austenite, EBSD, 3-dimensional atom probing, TEM

Corresponding author: Dr. N. Wanderka
Helmholtz Centre Berlin
Glienickerstr. 100
14109 Berlin
Germany
Tel.: + 49-30-8062-2079
Fax: + 49-30-8062-3059
e-mail: wanderka@helmholtz-berlin.de

1. Introduction

Precipitation hardened (PH) maraging steels have been developed for applications in environments requiring good mechanical properties (yield stress and fracture toughness) and high corrosion resistance. These alloys belong to the class of low-carbon steels that contain a substantial amount of Cr, Ni and Co together with small additions of Al, Ti and Mn. Depending on the application of these steels, their composition and their alloying elements is varied.

The high strength of maraging steels is obtained by a solution heat treatment followed by a tempering treatment typically between 673 K and 803 K. During tempering, precipitation of different intermetallic phases takes place. The variety of different precipitates depends on both the composition of maraging steels and on the heat treatment. Microstructural evolution, clustering, precipitation and hardening have been investigated in detail in many studies [1–7]. It has been shown that the intermetallic phases formed during ageing are not stable equilibrium phases. Prolonged tempering leads to coarsening of the precipitates and, in addition, to the formation of reverted austenite. Both adversely affect mechanical properties. In particular, it was found that the occurrence of reverted austenite has a negative effect on toughness [8]. The amount of the reverted austenite has been found to increase with ageing temperature and time [6,9]. The decrease in hardening observed during prolonged ageing is attributed to the formation of reverted austenite rather than to precipitate coarsening as has been shown in Ref. [10].

Because of the important influence of reverted austenite on mechanical properties at service temperatures the interest on austenite in maraging steels has been revieved recently. Different methods such as conventional transmission electron microscopy (TEM) [6,9] or non-destructive evaluation methods such as the magnetic Barkhausen emission technique [10] were successfully used to identify the reverted austenite.

The present steel termed *CORRAX* is one of the PH-maraging steels which can be used for the manufacture of micromoulds [11], of equipment for plastics and glass processing, extrusion dies, extruder screws for polymers, etc. Microstructural stability under service conditions is therefore of interest. In the present study the volume fraction of reverted austenite during prolonged ageing was estimated by X-ray and by electron backscatter diffraction (EBSD) analysis. Precipitation hardening and precipitated phases were studied by micro-hardness measurements and by TEM analysis, respectively. The composition of the intermetallic phase was analyzed by 3-dimensional atom probe tomography. The effect of precipitation hardening and of reverted austenite on the mechanical properties was evaluated.

2. Experiment

The nominal composition of the investigated steel *CORRAX* produced by *UDDEHOLM* is given in Table 1.

The *CORRAX* steelwas solution-heat-treated at 1123 K for 0.5 h and subsequently air cooled to room temperature. After this treatment, the samples were aged at 798 K between 0.25 h and 300 h.

Platelets of 1×1 mm² size were mechanically ground to a thickness of about 10 μm, mounted onto a 3 mm titanium ring appropriate for use in TEM, and then ion beam milled at room temperature with Ar^+ to electron transparency. The conventional TEM investigations were performed using a Philips CM30 microscope, operated at 300 kV and utilizing a double-tilt sample holder.

The samples for X-ray diffraction analysis, scanning electron microscope (SEM) investigations and for the micro-hardness tests were mechanically polished in several steps. For the final step a diamond suspension with a particle size of 1 μm was used. The SEM samples were additionally polished electrochemically at −15°C and 20 V voltage using an electrolyte containing 89.4% ethanol, 9.9% perchloric acid and 0.7% thiourea.

The XRD measurements were performed with a Bruker-AXS Powder diffractometer “D8 Advance” using a tube with Cu-K_α radiation and a double monochromator.

The Vickers micro-hardness measurements were determined with a micro-hardness tester (Paar Physica MHT-10) using a load of 2 N (HV 0.2) and a holding time of 15 s.

A three-dimensional atom probe (TAP, CAMECA) was used to study three dimensional distribution of alloying elements in the samples aged at 798 K. Specimens were prepared using standard techniques as described in Ref. 7.

The electron backscatter diffraction (EBSD) measurements were performed on a SEM (LEO GEMINI 1530) equipped with an Oxford Instruments HKL NordlysII detector. The voltage applied was 20 kV, and the probe current about 1 nA. The EBSD patterns were acquired and evaluated using the Oxford Instruments HKL software package CHANNEL5. EBSD maps were recorded with point-to-point distances of 50 nm and with recording durations of about 80 ms at each point.

3. Results and Discussion

3.1. Precipitation hardening

The Vickers micro-hardness evolution of the specimens after solution heat treatment (SHT) and after subsequent ageing at 798 K as a function of the ageing time is shown in Fig. 1. The micro-hardness value of 365 HV of the solution heat treated specimens is shown as a broad line which illustrates the error of this value. Specimens aged at 798 K show a sharp rise in micro-hardness up to 555 HV within the first 3 hours. The peak hardness of 578 HV was obtained after 12 h of ageing. This value corresponds to an increase of about 63% in micro-hardness, as compared with that directly after solid solution heat treatment. Beyond peak hardness there is a moderate decrease in hardness. Even after 300 h the hardness value is about 522 HV, which is still 43% higher than the value directly after solid solution heat treatment. As the mechanical properties are related to the microstructure, an increase of strength of this steel during ageing is mainly caused by very fine precipitates embedded in a solid solution matrix as is evident from the TEM images shown in Fig. 2b.

The structure of the fine precipitates formed at the beginning of ageing has not been identified successfully in TEM due to the extremely weak selected area electron diffraction (SAD) pattern, their diffuse diffraction intensity and the large number of defects in the martensite. Therefore, the specimen aged at 798 K for 100 h was chosen to show here. A representative example of the microstructure of the maraging steel exhibiting the typical lath-shaped martensite is shown in the bright-field TEM micrograph in Fig. 2a. The majority of these laths contain a high density of entangled dislocations. The corresponding SAD pattern of the marked section in Fig. 2a shows superlattice reflections within the [001] zone axis stemming from the matrix (inset in Fig. 2b). The dark field micrograph in Fig. 2b based on the [010] superlattice reflection shows fine coherent precipitates which correspond to a B2 (CsCl) superlattice structure.

In order to obtain quantitative measurements of precipitates and matrix compositions and the partitioning of the alloying elements atom probe (3DAP) tomography was used. 3DAP is suitable to study and analyze features on the nanometre scale. An example of such measurements from the specimen aged for 10 h is shown in Fig. 3. A three-dimensional reconstruction of Al atom positions within an analysed volume $9\times9\times60$ nm^3 is obtained. Several areas enriched in Al are clearly observed. Al was chosen as a representative element due to its precipitation during ageing. The same areas are also enriched in Ni, but depleted in Fe and Cr (not shown). The shape of the Al-enriched zones can be observed by rotating the region of interest. In Fig. 3a and 3b one part of the same investigated volume is presented with precipitates in two different orientations. From these figures it can be recognized that the precipitates have a plate-like structure. Their typical size is about $2\times6\times6$ nm^3. The shape and

the size of these precipitates are similar. All of these platelets are located in planes parallel to each other. The number density of the precipitates at this ageing state (near peak hardness) is about 2.1×10^{24} m^{-3}.

The concentration depth profiles for most significant elements (Fe(a), Ni(b) and Al (c)), are shown in Fig. 4. They were taken along the box with a cross section of 0.6×2 nm^2. This was selected in such a way as shown in Fig. 4d. The concentration depth profiles show sharp interfaces between matrix and precipitate. The width of the interfaces is about 0.5 nm. The precipitates contain 33 at.% Al, 37 at.% Ni and 28 at.% Fe. The Al content in the matrix of about 0.7 at.% is below the nominal composition of 3.39 at.%. The calculated volume fraction of precipitates is 11.4±0.5 %.

In this study the strain associated with coherent ordered plate-like precipitates in martensite proves to be the main source of hardening. A quantitative characterization of precipitates was possible by 3DAP measurements and the structure of precipitates was evaluated by TEM analysis. The high particle density indicates high nucleation rate. The homogeneous distribution of precipitates in the matrix indicates a high driving force for precipitation of this phase. Despite the similar composition of *CORRAX* and the other maraging steels reported in literature [1–5,7,13,14], the presence of only one intermetallic phase Ni-Fe-Al was found in the present steel. The hardened intermetallic phases obtained in Ref.'s [1–5, 7, 13] and [14] are mainly enriched in Ni and Ti or and Ni and Mo. The Ti-rich precipitates cannot be expected in the present steel because of the lack of Ti. Mo-rich precipitates were not detected in *CORRAX*. From the results of thermodynamic calculations reported in Ref. [14] for a similar steel the solubility of Mo in the matrix at 793 K is estimated to 0.6 at.%. Since the amount of Mo in *CORRAX* is only 0.79 at.%, the availability of Mo for precipitation from the matrix is also restricted.

3.2. Reverted austenite

In order to describe the formation of the reverted austenite and to calculate its volume fraction two complementary methods, namely XRD and EBSD analyses were used. The results of the XRD measurements of samples after solution heat treatment and ageing at 798 K for different times are presented in Fig. 5. It is evident that during this treatment at 798 K the changes in the intensity of the X-ray reflections are not significant. For the aged specimens, only a small increase in intensity of the fcc phase corresponding to austenite is visible. Superlattice reflections from the ordered intermetallic phase do not occur.

The measured diffraction pattern are fitted using calculated peak positions for the bcc and the fcc structure. The lattice parameters of both phases were evaluated and are listed in Table 2. Obviously, there is a difference in the bcc lattice parameters between the solution heat treated and the aged material. This difference can be explained by the fact that Al atoms with the largest atomic radius are rejected from the matrix during precipitation, leading to a shrinkage of the matrix lattice.

The intensity of the bcc (011) and the fcc (111) reflections were used to estimate the fraction of austenite in the alloy. The austenite volume fraction of 1.1±0.1 vol.% was constant in all aged samples, independent of the time. After solution heat treatment fcc-patterns also appear, but their intensity is lower and therefore the approximation of the austenite volume fraction contains a larger error: 0.5±0.2 vol.%. The determination of such a small amount was only possible because due to the different structure factors for bcc and fcc lattice. The scattering intensity of the fcc lattice is 4 times the intensity of the bcc lattice.

EBSD measurements were used to visualize the austenite and to calculate its volume fraction of samples after solution heat treatment and after subsequent aging for 3, 10, 100, and 300 h. EBSD pattern-quality maps of the samples are shown in Fig. 6. The austenite grains of the SHT sample reveal small sizes (Fig. 6). Their calculated volume fraction is smaller than 1vol. %. The average size of the austenite grains for the 10 h sample is substantially larger than for the other samples. The microstructure of the martensite in this micrograph also appears to be coarser. However, the volume fractions of the austenite for all samples (3, 10, 100, 300 h), except for SHT, are similar (see Table 3). It was found that the austenite forms preferentially at the martensite lath-boundaries rather than within the martensite lath. The orientation relationship between martensite and austenite was found to be of the Kurdjumov-Sachs type $(111)_{fcc} \parallel (011)_{bcc}$ with $[10\text{-}1]_{fcc} \parallel [11\text{-}1]_{bcc}$. The same relationship between martensite and austenite was reported in [9].

The volume fraction of austenite measured by EBSD is higher than evaluated by X-ray diffraction. The differences in the volume fraction between EBSD and X-ray diffraction could be due to heterogeneities of the austenite distribution and to the detection limitation of X-ray diffraction. Both may influence the result. However, in both cases the values of the austenite volume fractions remain constant and very low, independent of ageing time.

The chemical composition of the austenite was determined in TEM using energy-dispersive X-ray microanalysis. The amount of Ni in the austenite was found to be twice (15 to 18 at.%) of the nominal composition (~ 8.5 at.%). Similar relations of the Ni composition in the

austenite after ageing were reported in 18Ni (350) maraging steel [9]. Some austenite grains in *CORRAX* also contain large amounts of Al (~ 12 at.%) as was obtained in the sample aged for 100 h. One possible explanation of the high amount of Al is that during prolonged ageing the intermetallic precipitates near the grain boundaries dissolve, resulting in a local enrichment of Ni and Al at preferred sites where austenite reversion is initiated.

The volume fraction of austenite and micro-hardness as a function of ageing time are shown in Fig. 7. A drop in micro-hardness is observed for ageing times larger than 20 h and can be explained by coarsening of the intermetallic phase and by relaxation of dislocations at prolonged treatment. A similar micro-hardness course (nearly the same maximum hardness at the same time) has been reported for a M250 maraging steel [10]. However, in that steel the volume fraction of austenite increases rapidly at 30 h [10] and reaches a value of 32 vol.% at 100 h, whereas in *CORRAX* it is still nearly unchanged (1-2 vol.%) throughout ageing up to 300 h. The observed delay in the formation of reverted austenite in *CORRAX* may be explained by the lower amount of Ni (~ 9 at.%) as compared to the M250 maraging steel (about 18 %), because the austenite is enriched in austenite-stabilizing Ni.

Finally, the austenite amount (1-2 vol.%) found in the present study is in good agreement with a value of predicted equilibrium phases for 798 K (fcc austenite 2.5 vol.%) calculated using “Thermocalc” (Database NiFe) [15].

Conclusions

The present study of the microstructure and mechanical properties of *CORRAX* maraging steel indicates that this steel is of technological and practical importance. The amount of reverted austenite is about 1-2 vol. %, which is in good agreement with a calculated value of 2.5 vol.%. The delay of the formation of reverted austenite during prolonged ageing up to 300 h at 798 K may be due to the composition (absence of Ti) of this steel. The micro-hardness decrease can be explained mainly by coarsening of the fine intermetallic Ni-Fe-Al phase of B2 structure as well as dislocations relaxation.

References

[1] K. Stiller, F. Danoix, A. Bostel, Appl. Surf. Sci. 94/95 (1996) 326-333

[2] K. Stiller, M. Hättestrand, F. Danoix, Acta Mater. 46 (1998) 6063-6073

[3] Z. Guo, W. Sha, D. Vaumousse, Acta Mater. 51 (2003) 101-116

[4] M. Hättestrand, J.-O. Nilsson, K. Stiller, P.Liu, M. Andersson, Acta Mater. 52 (2004) 1023-1037

[5] E.V. Pereloma, A. Shehter, M. Miller, S.P. Ringer, Acta Mater. 52 (2004) 5589-5602

[6] U.K. Viswanathan, G.K. Dey, V. Sethumadhavan, Mater- Sci. & Eng. A 398 (2005) 367-372

[7] H. Leitner, H. Clemens, S. Höring, N. Wanderka, J. Banhart, P. Staron, B. Jamnig, Zeitschrift für Metallkunde **95;** (2004); 644-649

[8] C.A. Pampillo, H.W.Paxton, Metall. Trans. A31 (1972) 2895-2903

[9] X. Li, Z. Yin, Mater. Letters 24 (1995) 239-242

[10] K.V. Rajkumar, S. Vaidyanathan, A. Kumar, T. Jayakumar, B. Raj, K.K. Ray, J. Magnet. & Magnet. Mater. 312 (2007) 359-365

[11] T. Gietzelt, L. Eichhorn and K. Schubert, Adv. Eng. Mater. 8 (2006) 33-37

[12] Data sheet of steel Corrax by “Böhler-Uddeholm Deutschland GmbH”: http://uddeholm.de => Produkte/Service => Produkte => Kunstoffformen-stähle => Corrax (Download)

[13] W. Sha, A. Cerezo and G.D.W. Smith, Metall. Trans., 24A (1993) 1241-1249

[14] A. Gemperle, J. Gemperlova, W. Sha and G.D.W. Smith, Mater. Sci. & Technol. 8 (1992) 546-554

[15] Thermo-Calc Software, AB, SE-113 47 Stockholm, Sweden

Figure captions

Fig. 1: Vickers micro-hardness as a function of ageing time for *CORRAX* steel after solution heat treatment (SHT) and subsequent ageing at 798 K.

Fig. 2: a) Bright-field TEM micrograph showing the typical martensitic lath morphology; b) Dark-field micrograph imaged with the [010] superlattice pattern showing the precipitates in bright contrast and oriented in [020] direction. The corresponding SAED pattern in b) shows the superlattice reflections of the B2 (CsCl) structure.

Fig. 3: 3D reconstruction of the aluminium atom positions of *CORRAX* samples after ageing at 798 K for 10 h. In order to observe the morphology of the particles, one part of the same investigated volume with precipitates is presented in two different directions a) and b).

Fig. 4: Concentration depth profiles of *CORRAX* steel for Fe (a), Ni (b) and Al (c) after of aging at 798 K for 10 h. The vertical dashed lines marking the interface between matrix and precipitates. The position of the box used for the concentration measurements is shown in (d). The cross section of the box is 0.6 x 2 nm². The step size for the concentration measurements is 0.2 nm.

Fig. 5: Results of the XRD measurements of *CORRAX* samples after aging for different times at 798K and after solution heat treatment. The results are given as standardised intensity showing the reflexes of the bcc (martensite) and the fcc (austenite) phase. The amount of the fcc – phase approximated by the intensity of the main peaks of both phases is constant 1.1±0.1 vol.%

Fig 6: EBSD pattern-quality maps with austenite precipitates highlighted in yellow.

Fig. 7: Vickers micro-hardness and volume fraction of austenite as a function of ageing time at 798 K for *CORRAX* steel.

Figures

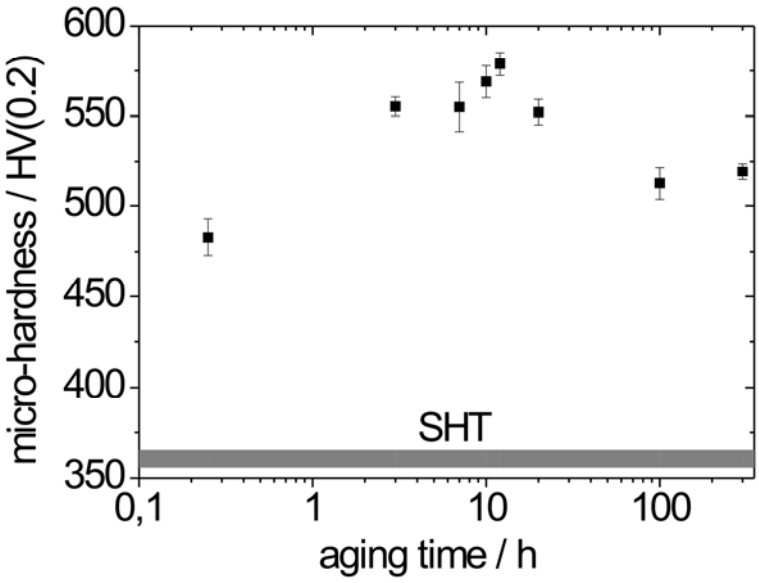

Fig. 1

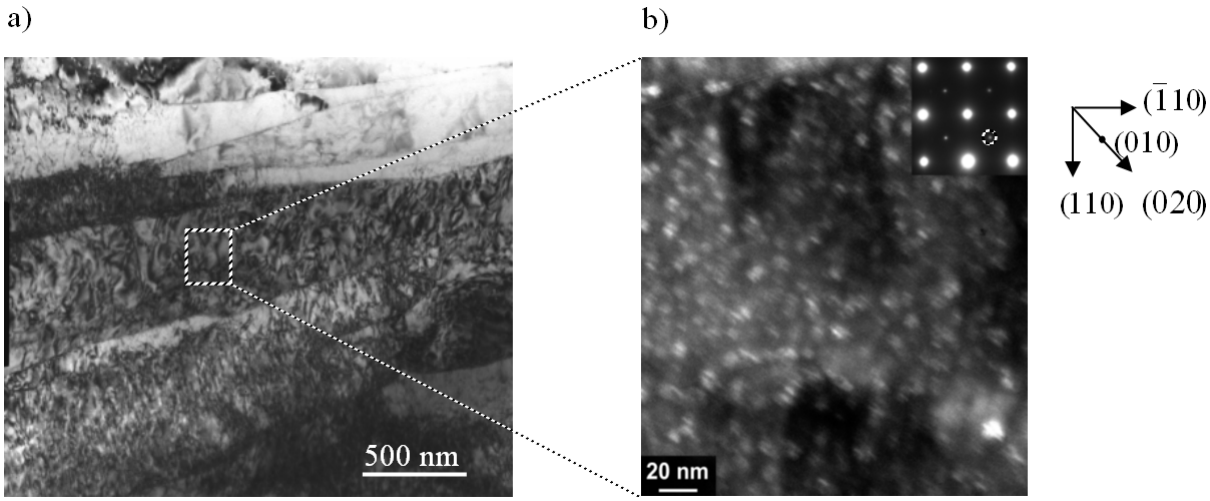

Fig. 2

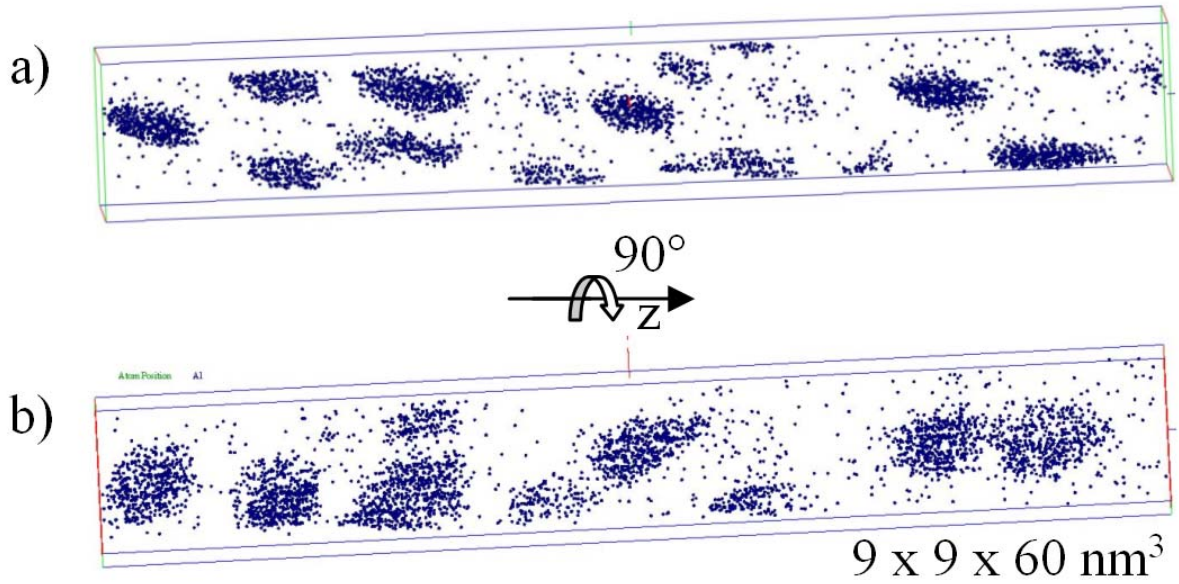

Fig. 3

(a)

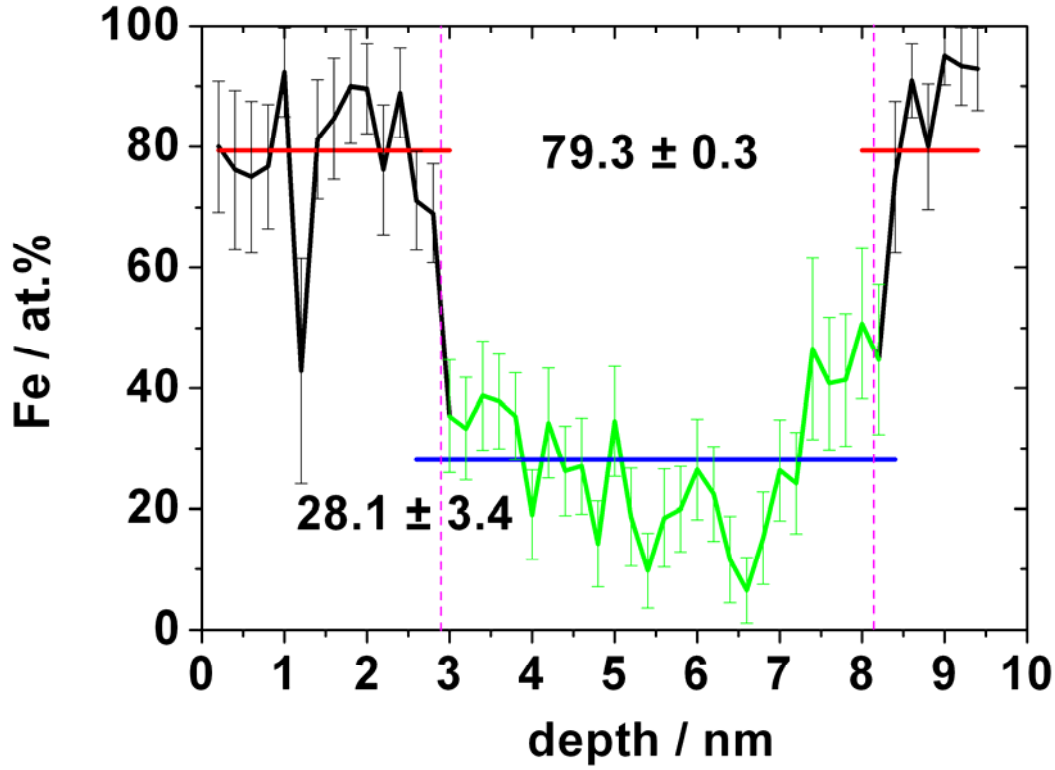
Fe / at.%
depth / nm
79.3 ± 0.3
28.1 ± 3.4
0
20
40
60
80
100
0
1
2
3
4
5
6
7
8
9
10

(b)

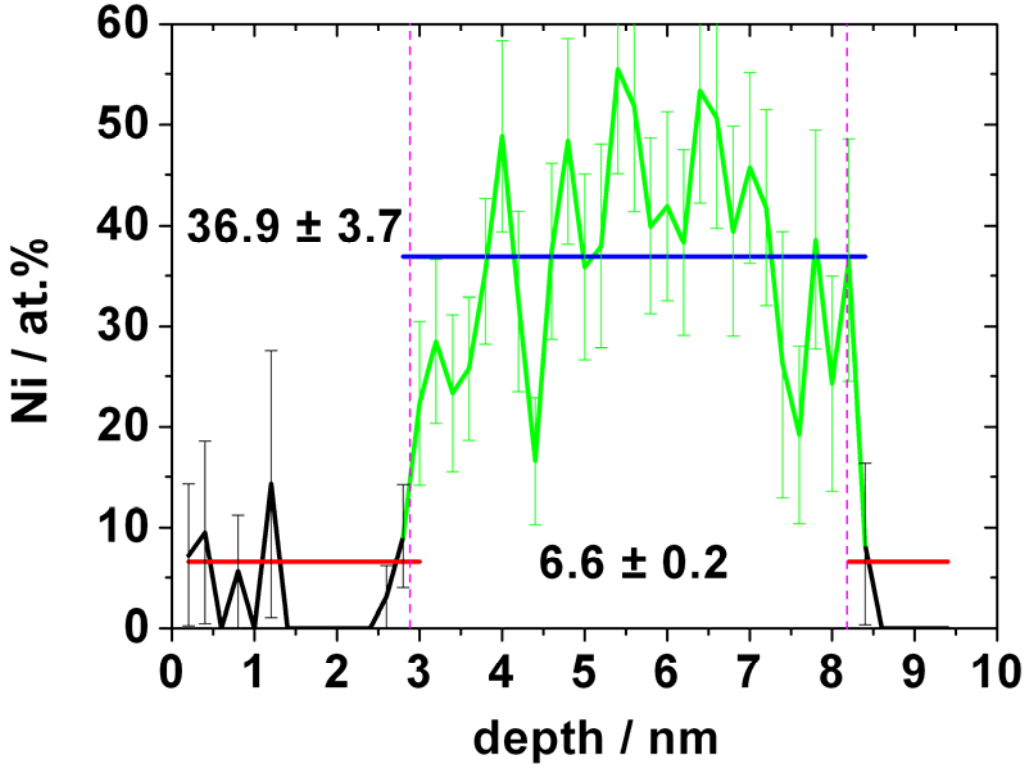
Ni / at.%
depth / nm
36.9 ± 3.7
6.6 ± 0.2
0
10
20
30
40
50
60
0
1
2
3
4
5
6
7
8
9
10

(c)

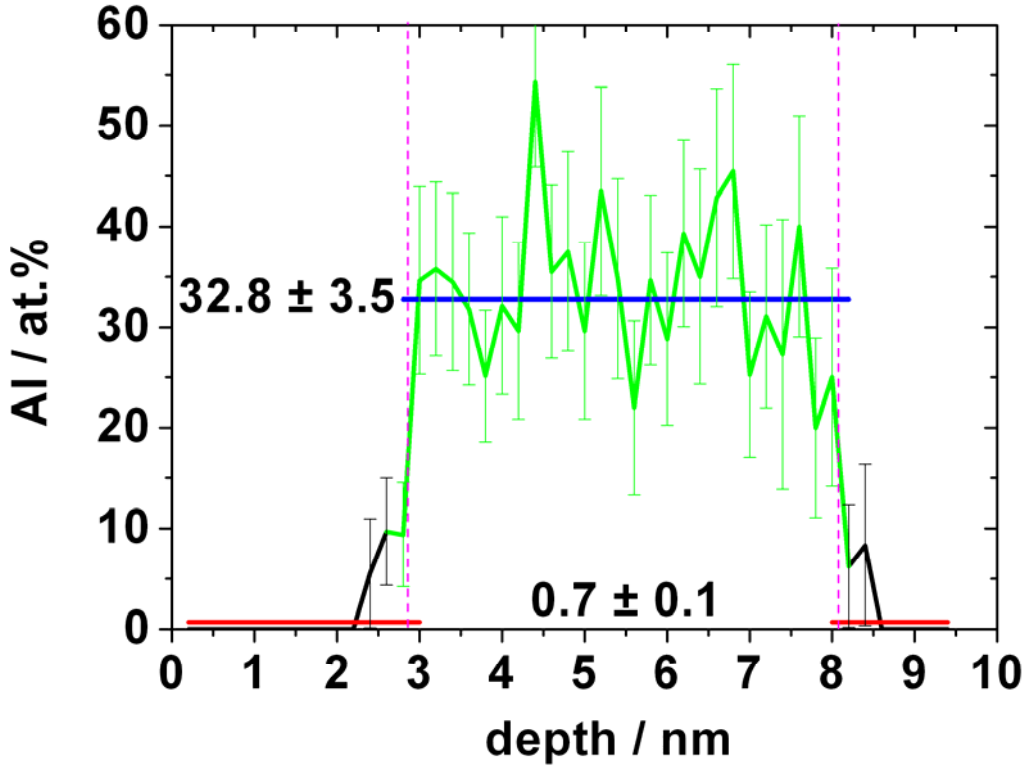

(d)

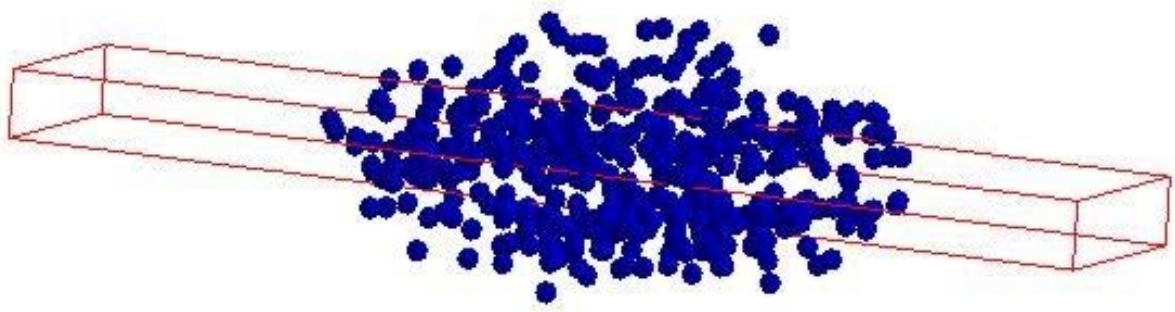

Fig. 4

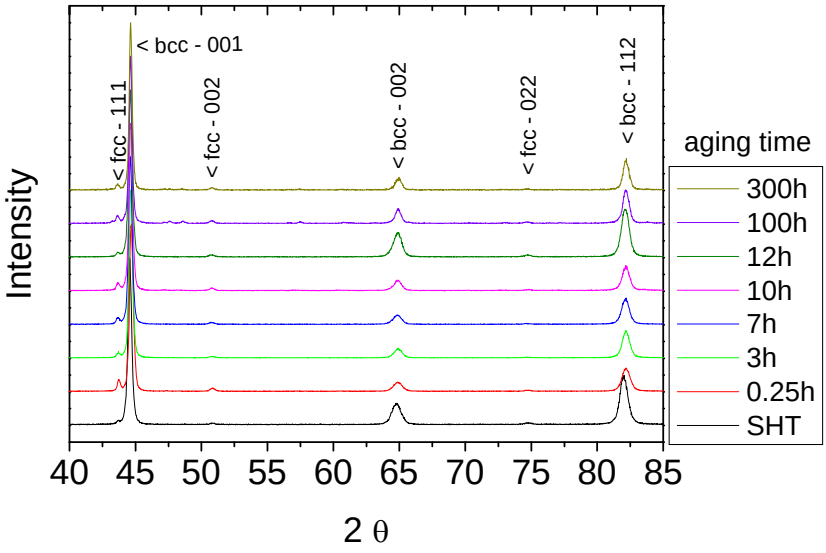
< bcc - 001
< fcc - 111
< fcc - 002
< bcc - 002
< fcc - 022
< bcc - 112
Intensity
aging time
300h
100h
12h
10h
7h
3h
0.25h
SHT
40 45 50 55 60 65 70 75 80 85
2 θ

Fig. 5

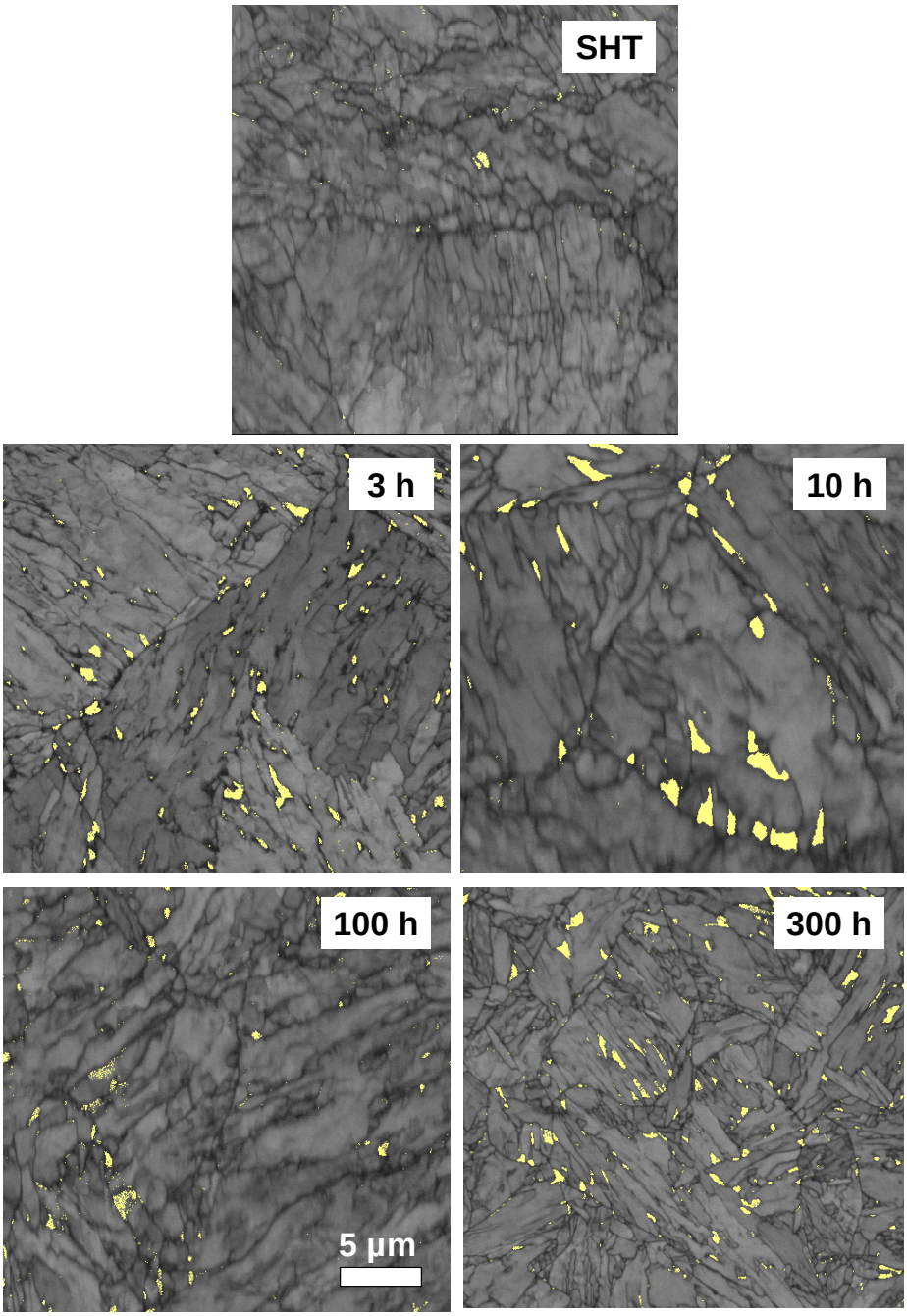

Fig. 6

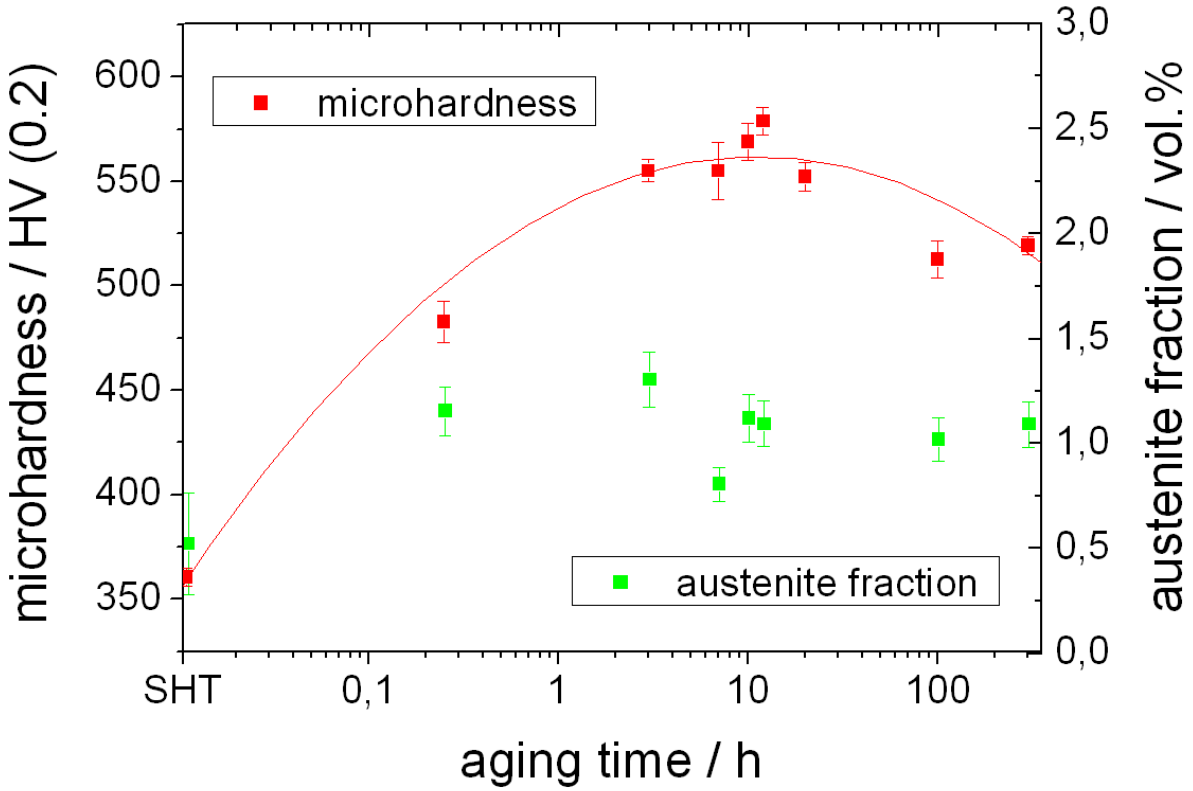
microhardness / HV (0.2)
austenite fraction / vol.%
aging time / h
microhardness
austenite fraction
600
550
500
450
400
350
3,0
2,5
2,0
1,5
1,0
0,5
0,0
SHT
0,1
1
10
100

Fig. 7

Tables

Table 1. Nominal composition of the investigated alloy *CORRAX*.

Table 2: Lattice parameters of bcc matrix and fcc austenite.

Table3: Volume fractions of the austenite in the samples studied, as determined by EBSD.

Table 1

CORRAX	Fe	Cr	Ni	Al	Mo	Mn	Si	C
wt.%	74.97	12.12	9.14	1.67	1.38	0.39	0.30	0.03
at.%	73.46	12.76	8.52	3.39	0.79	0.39	0.58	0.11

Table 2

lattice		lattice constant / Å
bcc	SHT	2.878
	after ageing	2.874
fcc		3.591

Table 3

Ageing time / h	Volume fraction austenite / %
SHT	< 1
3 h	2.1
10 h	1.8
100h	2.2
300 h	2.0